ASSESSMENT OF THE IMPACT OF SHRIMP AQUACULTURE IN NORTHEAST BRAZIL: A REMOTE SENSING APPROACH TO COASTAL HABITAT CHANGE DETECTION

By

Adam G. Zitello

Date: _____

Approved:

_____
Dr. Patrick N. Halpin, Advisor

Masters project submitted in partial fulfillment of the
requirements for the Master of Environmental Management degree in
the Nicholas School of the Environment and Earth Sciences of
Duke University

2007

Abstract:
Aquaculture is the fastest growing sector of food production in the world. However, rapid expansion of shrimp aquaculture ponds may induce potentially detrimental changes in extent and health of coastal habitats utilized by migratory shorebirds. The aim of this work is to describe the landscape changes that occurred between 1990 and 2006 in coastal Northeast Brazil as a result of increased shrimp pond development. A suite of remote sensing techniques was employed to process Landsat and ASTER imagery at three separate time periods (1990, 2000 & 2006) and generate land cover maps for each time period. Post-classification change detection analysis revealed critical conversions between identified coastal habitat types in Northeast Brazil. The results of this study revealed a substantial growth of shrimp aquaculture facilities on the northern coast of Northeast Brazil between 1990 and 2006. Contrary to the literature, the expansive tidal salt flats in the study area, not mangrove forests, are experiencing the greatest destruction as a result of shrimp aquaculture. Research and management efforts should be directed at determining the extent of utilization of these salt flat areas by migratory shorebirds.

Table of Contents

1. Introduction

Aquaculture is the fastest growing sector of food production in the world. The Food and Agriculture Organization (FAO) of the United Nations (2006) reports that aquaculture accounts for almost 50% of the world's food fish. Aquaculture has the greatest potential to meet the growing demand of aquatic food that will arise from an expected population increase of 1.5 billion people in 2020. In order to maintain the current per capita consumption, an additional 40 million tons of aquatic food will be required by 2030 (FAO 2006). Mounting scientific evidence indicates that dramatic declines in many natural fish stocks are occurring. Capture fisheries are not capable of providing fish to an additional 1.5 billion people, considering FAO already lists 89% of the ocean's wild fish stocks as moderately, fully or over-exploited.

In addition to meeting global consumption needs, aquaculture, particularly shrimp farming, has become an increasingly important economic activity. In recent years, high value and market demand by mainly affluent consumers in developed countries has lead to rapid expansion of shrimp aquaculture throughout Asia and Latin America. In 1999, shrimp aquaculture only represented about 2.6% of total global aquaculture, but accounted for 16.5% of the total revenue at a value of about $6.7 billion (World Bank et al. 2002). Considerable private and public sector investment has induced an annual average increase in cultured shrimp production of about 5-10% since the 1990's.

Despite the favorable conditions of land availability and climate, the Brazilian shrimp industry has taken longer to develop than other countries'. Between 1972 and 1984, private and public investors tried on numerous occasions to initiate a shrimp farming industry in Brazil, but obstacles in species selection and economic instability proved disastrous. For the next fifteen years, the industry made incremental improvements in culture techniques but was unable to capitalize on the shrimp culture boom experienced in other Latin American countries. In 1990, a currency devaluation and disease outbreak in Pacific coastal farms in other Latin American countries opened the door to international markets (Moles & Bunge 2002). Production doubled every year between 1997 and 2002 as a result of pond expansions and increased stocking densities (Moles & Bunge 2002). Shrimp aquaculture is expanding rapidly in Brazil today. There are over 100 farms operating under varying capacities in the region of Northeast Brazil.

Given the profitability and demand of cultured shrimp, Northeast Brazil's expansive coastal lands may undergo significant development by shrimp aquaculture facilities.

The coast of Brazil has also been recognized as one of the most important areas in the migration of small shorebirds. Every year, thousands of migratory shorebirds of all species travel from North America to their wintering grounds as far South as Tierra del Fuego. The survival of many migratory shorebird species directly depends on the quality and abundance of stopover sites along their flyway. The extensive mangrove forests and intertidal areas of Northeast Brazil's shoreline provide food resources and shelter for migrating populations. With the development of shrimp aquaculture have come reports that many coastal habitats in Northeast Brazil are being destroyed.

The objectives of this study in coastal Northeast Brazil are to (1) map the location of shrimp aquaculture facilities in 1990, 2000 and 2006; and (2) determine the coastal habitats of significance to migratory shorebirds that have been lost to aquaculture expansion over the same time period.

2. Study Area

The study area is located on the northern coast of Northeast Brazil (Figure 1) and spans the jurisdiction of four different Brazilian states; Marahnao, Piaui, Ceara and Rio Grande do Norte. The greater than 700 kilometers (km) of shoreline frames an area of 12,386,294 hectares (ha) between latitude 2º15´N - 6º33´N and longitude 43º20´W - 35º60´W. The exceptionally flat macrotidal region is dominated by microtopography and inundated by large vertical tidal changes. Dense mangrove forests backed by extensive tidal salt flats dominate the intertidal portions of the landscape. Northeast Brazil has a semi-arid climate with two significant seasons, the wet season from January to August and the dry season

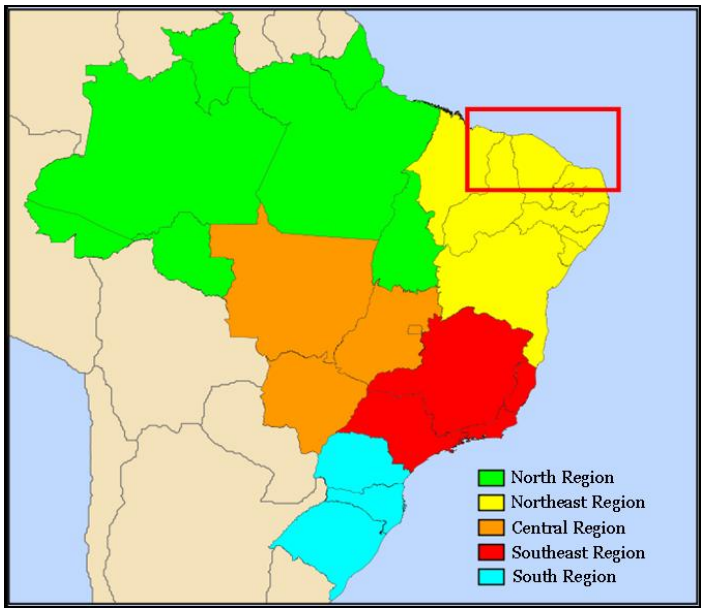

Figure 1. Overview of Brazilian regions and the study area defined by a box

from September to December. The climate allows for several larger rivers that flow from south to north in the Atlantic Ocean, but none compare in magnitude to the Amazon River to the west of the region. Although some coastal forests are present, the study area's upland is primarily covered by scrub and shrub vegetation.

3. Methods

This study was designed to assess the landscape changes induced by shrimp aquaculture development on the northern coast of Northeast Brazil between 1990 and 2006 utilizing remote sensing procedures. A variety of classification techniques were utilized to create land cover maps with significance to migration of shorebirds. The change detection approach employed was a post-classification comparison of land cover maps displayed in a change detection matrix.

3.1. Imagery

Satellite imagery of Northeast Brazil was acquired for three different time periods by three different sensors. The 1990 time period images were acquired by Landsat 5 Thematic Mapper (TM); 2000 time period images were from Landsat 7 Enhanced Thematic Mapper + (ETM+); and 2006 images were from Advanced Spaceborne Thermal Emission and Reflectance Radiometer (ASTER) visible and near-infrared (VNIR) suite. Landsat spectral band 6 was omitted because it represents the thermal portion of the electromagnetic spectrum and is limited in habitat mapping. Anniversary dates for all images were considered sufficiently close to exhibit similar phenological characteristics in the vegetation.

Fundamental differences exist between the two Landsat sensors and the ASTER VNIR sensor. These sensor differences did not hinder analysis between the time periods, but

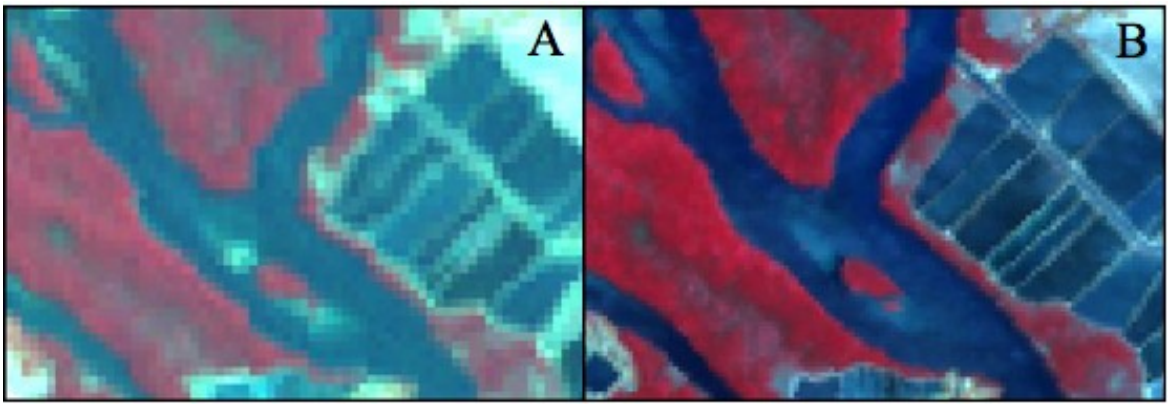

Figure 2. Spatial resolutions differ between Landsat (panel A) and ASTER (panel B)

were considered during the design of analytical methods. As seen in Figure 2, spatial resolution is twice as great in ASTER data (15 m cell size) as with Landsat data (30 m cell size). Spectral resolutions also differ, with Landsat recording 7 bands and ASTER only providing 3 bands. Fortunately, bands 2, 3 and 4 of the Landsat sensor occupy the same spectral ranges as bands 1, 2 and 3 of the ASTER sensor, which allows comparable RGB display and analysis to be conducted across sensors. The swath width of a Landsat scene is 185 km compared to the 60 km of an ASTER scene. As such, Landsat scenes constitute a continuous coverage throughout the entire study area while ASTER scenes are only present in critical areas of interest. As a result of the less than complete ASTER imagery coverage over the study area, analysis methods varied for change detection between 1990 to 2000 and 2000 to 2006.

Budgetary constraints limited Landsat data acquisition to free images from the University of Maryland's Global Land Cover Facility (GLCF). In an attempt to use anniversary dates and cloud-free data, images were selected that were within a few years of each desired time period. As a result, 1990 time period images were actually acquired between 1988 and 1993 and 2000 time period images were acquired between 1999 and 2001.

3.2. Radiometric Correction

Detecting landscape changes from remote sensing of the earth's surface requires a consistent depiction of object illumination across time and space. Ideally, the amount of energy recorded by a remote sensing system is an accurate representation of the actual energy being reflected from a feature on Earth's surface. Unfortunately, there are two primary points at which error may enter into the data collection system. The first case is when an aging remote sensing instrument's characteristics have changed since launch and the internal calibrator is no longer properly functioning (Chander and Markham 2003). The second is when the intervening atmosphere between the terrain of interest and the remote sensing system prohibits the entire amount of energy to reach the sensor; this is referred to as atmospheric attenuation (Jensen 1996). Pre-processing steps were incorporated into this analysis in order to correct radiometric degradation of Landsat imagery. These conversions improved the comparison of scenes taken at different dates and by different sensors.

Literature has shown that the assumption of constancy of internal lamp radiance over time is not valid (Markham et al. 1998)(Helder et al. 1998). Chander and Markham (2003)

proposed a radiometric calibration technique that uses rescaled satellite gain and bias values modified from past calibration procedures in the National Landsat Archive Production System (NLAPS). Application of the following equation to Landsat TM and ETM+ Level 1 data will result in a conversion from digital number (DN) to at-sensor spectral radiance:

$$L_\lambda = G_{rescale} * Q_{cal} + B_{rescale} \qquad \textit{Eq. 1}$$

where

L_λ = spectral radiance at the sensor's aperture in W/(m² · sr · μm) (at-satellite radiance)

$G_{rescale}$ = gain rescaling factor in W/(m² · sr · μm) (see Appendix 1)

Q_{cal} = quantized calibrated pixel value in DNs

$B_{rescale}$ = bias rescaling factor in W/(m² · sr · μm) (see Appendix 1)

Markham and Chander's conversion to at-sensor radiance accounts for radiometric inconsistencies arising from inaccurate internal calibration, however considerable radiometric error still existed due to atmospheric effects. When solar radiation enters Earth's atmosphere it is selectively scattered and absorbed by gases and aerosols. The total energy loss due to scattering and absorption is referred to as atmospheric attenuation (Jensen 1996). It is essential to correct atmospheric effects when employing a classification and change detection approach because images must be normalized across time and space.

Dark object subtraction (DOS) is one of the simplest and most widely used atmospheric corrections applied before image classification. The approach assumes that an object exists in the image for which there is little or no surface reflectance. The minimum value in the image's histogram should correspond to the dark object. In theory, any energy recorded at this dark object is a result of atmospheric attenuation and is subtracted from every pixel throughout the image. Song et al. (2001) derived an algorithm that utilizes a dark object subtraction to convert at-satellite radiance to surface reflectance. Application of the following adaptation of Song et al.'s DOS Method 1 effectively removes radiometric errors induced by atmospheric attenuation in Landsat imagery:

$$p = \frac{\pi(L_\lambda - L_p)}{T_v(E_0)} \qquad \textit{Eq. 2}$$

where

$p =$ surface reflectance

$L_\lambda =$ at-satellite radiance (from *Eq.1*)

$L_p =$ path radiance (from *Eq.1*)

$T_v =$ atmospheric transmittance from target towards sensor (see Appendix 2)

$E_0 =$ exoatmospheric solar constant (see Appendix 3a & 3b)

with

$$L_p = \frac{L_{\lambda\min} - 0.01 * (E_0 * \cos(\theta_z) T_z + E_{down})}{\pi} \qquad \textit{Eq. 3}$$

where

$L_{\lambda\min} =$ minimum L_λ value with at least 10,000 pixels

$\theta_z =$ solar zenith angle

$T_z =$ atmospheric transmittance in the illumination direction (see Appendix 2)

$E_{down} =$ downwelling diffuse irradiance (see Appendix 2)

DOS Method 1assumes no atmospheric transmittance loss ($T_v = T_z$) and no diffuse downward radiation at the surface ($E_{down} = 0$). The resulting scenes were stitched together into 1990 and 2000 radiometrically corrected Landsat mosaics using ERDAS Imagine's Mosaic Tool. These mosaics were the basis of the remaining processing steps mentioned herein.

3.3. Land Cover Classification

An expert consultation and literature review were conducted to determine the coastal habitats critical to shorebird migration through Northeast Brazil. This effort resulted in identification of four critical habitats (mangrove, salt flat, sand dune, aquatic surface) and a fifth land cover type corresponding to shrimp pond development. A variety of methods were

employed to individually classify these five categories and ultimately create coastal land cover composite maps for 1990 and 2000. A land cover composite was not created for 2006 due to gaps in quality cloud-free ASTER imagery over the study region. The following sections document the methods used to classify each land cover type.

3.3.1. Shrimp Aquaculture Ponds

Shrimp aquaculture ponds are one of the most distinct landscape features on the coast of Northeast Brazil. Unfortunately, spectral classification of shrimp ponds leads to difficulties in differentiating between near-shore seawater and aquaculture water. Similar to Beland et al. (2006), no spectral signature was determined to be unique in any of the six reflective Landsat bands for most shrimp ponds. Beland et al. (2006) suggested that this problem might be explained by a high content of organic matter in the ponds. The level of organic matter is directly related to the amount of unconsumed feed, shrimp stocking densities, organic waste and time of harvest cycle. All of these factors have likely contributed to aquaculture waters having similar suspended organic matter to near-shore ocean waters. In order to improve classification accuracy, the shrimp aquaculture class was created by visual interpretation and manual on-screen digitization.

With most aquaculture facilities implementing semi-intensive methods, average individual pond sizes range from 2 to 30 ha. However, there is a large diversity of farming systems and individual farms varied considerably in their layout and number of ponds. Regardless of the aquaculture technique adopted by the individual farms, there are several distinguishing characteristics of all shrimp aquaculture complexes. This study refined Daldegan et al.'s (2006) summary of key criteria for the identification of shrimp ponds when visual interpretation is employed:

- Ponds are standard geometric forms, usually rectangular.
- Ponds are located with proximity to the coastline.
- Ponds will occur in areas of little topographic relief, usually at or near sea level.
- Ponds are located with proximity to tidal waterways.
- Ponds are connected to tidal waterways by drainage canals.

Using these criteria, imagery displayed as false color was visually scanned at a scale of 1:50,000 to locate shrimp ponds.

After visual identification of a shrimp pond was made, ESRI's ArcGIS 9.2 editing environment was used to digitize the boundary of a shrimp aquaculture complex at a scale of 1:20,000. It is important to note that the entire footprint of an aquaculture facility was contained within the digitized boundaries, not just the ponds themselves. This effectively included area where:

- natural vegetation was disturbed by pond construction,
- natural vegetation was absent due to possible pond expansion,
- channels were dug for pond drainage,
- pond dikes were built to retain aquaculture waters, and
- ponds have been abandoned.

Aquaculture complex polygons were initially created in ESRI shapefile format, but were converted to ESRI raster grids to be used in the creation of land cover composites.

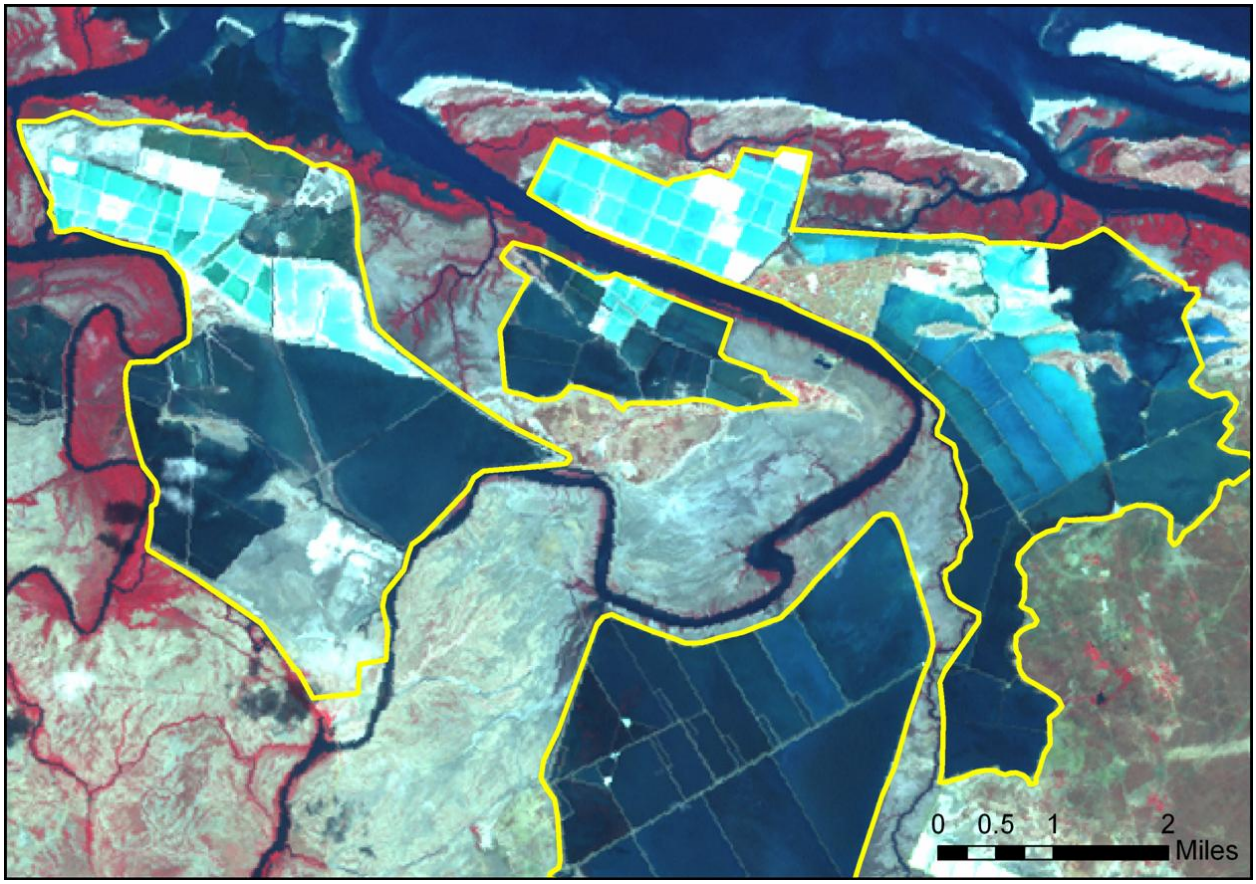

Figure 3. A false color ASTER image displaying shrimp pond boundary delineation at a scale of 1:50,000

3.3.2. Mangrove Forest

Mangrove forests prosper in the warm equatorial waters and low gradient coastal plains of Northeast Brazil. Mangroves inhabit the brackish area where the saltwater of the ocean and freshwater of the river mix in tidal waterways that are sheltered from wave action (Shoobridge 2004). Mangroves may penetrate as far inland as the limit of the salt wedge in tidal rivers will allow, which as suggested by experts (Cintron 2006), may be as far as 10-20 km upstream in Northeast Brazil. As a result, mangrove forests were only considered if they occurred within a 20 km buffer from the nearest shoreline.

Mangroves are generally easily recognizable on remotely sensed imagery by their dark and uniform canopy with few gaps or bare areas. A band of taller trees is usually found along tidal channels while canopy height will begin to taper at the edges of stands (Cintron & Schaeffer 2001). As distance from tidal waterway increases, tidal flushing decreases and mangroves become sparse and stunted. This area at extreme margins was often difficult to classify and was regularly omitted from the mangrove land cover category.

An unsupervised classification of the Landsat imagery for both 1990 and 2000 was used to create data layers of mangrove forest coverage. Unsupervised classification is a computer automated process whereby numerical operations are performed that search for natural groupings of the spectral properties of pixels in multispectral feature space without direct human intervention. The ISODATA (Iterative Self-Organizing Data Analysis Technique) clustering algorithm was processed in Leica Geosystems' ERDAS Imagine remote sensing software package. Parameters were set to begin clustering along the principal axis to produce 40 classes at a convergence level of 95% with a maximum of 25 iterations. Several mangrove classes were identified by visual comparison to the original Landsat imagery displayed in false color, then merged into a single mangrove thematic class. The resulting mangrove classification was smoothed by a 5 x 5 majority filter in order to eliminate classified raster cells that occurred in isolation. In other words, a sliding square window of 5 pixels on a side was passed over the entire classification looking for cell values of highest frequency. Genuine mangrove cells were left intact by the operation because of the spatial continuity of mangrove stands.

Rationale is provided in Green et al. (1998) for employing the conceptually simple unsupervised classification method while more complex approaches have been documented in the literature to classify mangroves using Landsat imagery. In summary, Green et al. found that

visual interpretation and Normalized Difference Vegetation Index (NDVI) classification performed the worst with overall accuracies of 42% and 57%, respectively. Both unsupervised and supervised classification processing methods produced an overall accuracy of more than 70%, but there was no significant difference between the two classification types. The most accurate classification of Landsat data (92%) was obtained using a Principal Components Analysis (PCA). Given the extensive area of this study and overall accuracy required, an unsupervised classification was deemed most cost effective in terms of processing time and data storage.

3.3.3. Salt Flat

The combination of Northeast Brazil's low gradient slope, macrotidal coastal margins and semi-arid climatic condition has created extensive tidal salt flats in the study area. Tidal salt flats, or apicum as they are referred to regionally, are hypersaline flatlands where salts are precipitated due to high evapotransportation and infrequent tidal flooding. Salinity levels in these salt flats regularly exceed the physiological tolerance of most plant species and the substrate is left bare or sparsely vegetated (Cintron & Schaeffer 2001). Brazil's salt flats usually develop between the Mean High Water Spring (MHWS) line and the upland tidal boundary. This tidal zone regularly occurs just behind the landward boundary of mangrove forests and is often considered in the literature to be part of the mangrove system (Figure 4).

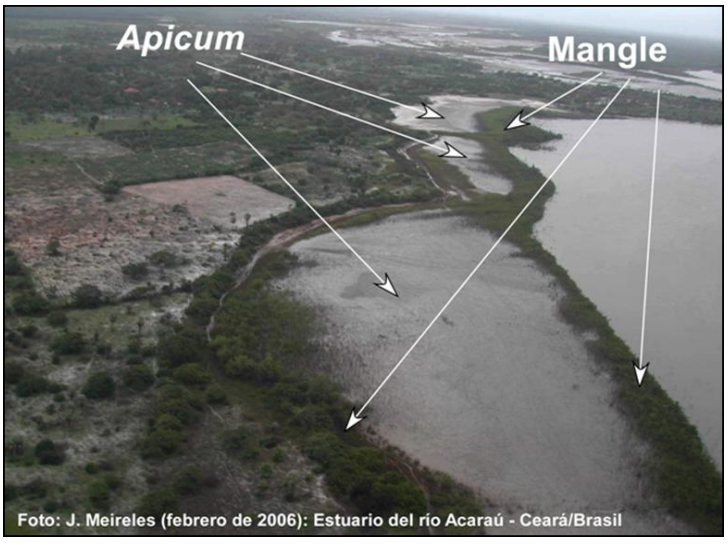

Figure 4. Aerial photo exhibiting the interconnection of mangrove and salt flat systems

The salt flat classification was derived in much the same manner as that of the mangrove classification. The initial unsupervised classification using an ISODATA algorithm (described in Section 3.3.2.) was compared to the original radiometrically corrected Landsat imagery. Several salt flat classes were identified using visual interpretation and merged into a single salt flat classification. Again, a

5 x 5 majority filter was applied to the combined salt flat classification in order to eliminate isolated cells that did not logically exist on the landscape.

3.3.4. Sand Dune

The northern coast of Northeast Brazil is covered by some of the most extensive coastal dune habitats in the world. Reaching as far inland as 10 km; these dune fields comprise nearly the entire coastline between the mangrove-lined river mouths of this region. Individual dunes range from 5 to 23 m in height and are rarely vegetated. The prevailing eastern winds from August to January are causing some individual dunes to migrate at a rate of 20 to 24 m per year (Barbosa & Dominguez 2004). This rapid Aeolian sedimentation is displacing the pre-existing scrub vegetation upland, establishing an abrupt boundary between distinctly different habitats (Figure 5). This phenomenon has created such a unique habitat condition that the World Wildlife Fund has established the Northeastern Brazil Restingas as one of the world's terrestrial ecoregions (World Wildlife Fund 2007).

The coastal sand dunes provide a distinct spectral signature, which aids in the ease of classification of this land cover type. Unlike adjacent areas covered by vegetation or water, this dry bare substrate has almost complete reflectance in the visible spectral bands of Landsat imagery. Sand dune classification was generated by once again combining several unsupervised classification categories into one thematic class. Refer to descriptions in sections 3.3.2. and 3.3.3. of this report for further description of the methodology.

Figure 5. The habitat contrast created by encroachment of sand dunes into scrub/shrub vegetation

3.3.5. Aquatic Surface

The aquatic surfaces land cover classification is a general category that represents all surfaces landward from the Mean High Water Line (MHWL) predominately covered by standing water. Features included as aquatic surfaces are rivers of at least 30 m in width, lakes, reservoirs, estuaries and bays. Any partially vegetated aquatic areas, including both coastal and freshwater wetlands, were not considered aquatic surfaces for the purpose of this classification.

A technical document authored by Earth Satellite Corporation (2004) was used to guide the classification of aquatic surfaces. A series of band ratioing, thresholding and conditional addition procedures were implemented in ESRI's ArcGIS 9.2 software package. The first process performed on the radiometrically corrected Landsat imagery was applied by the following Short Wave Infrared (SWIR) formula:

$$\frac{(Band7 * Band5)}{(Band7 + Band5)} \qquad \textit{Eq. 4}$$

This band ratio takes advantage of SWIR Bands' 5 and 7 ability to measure water and soil moisture. This formula was useful in differentiating the urban areas that are spectrally similar to water such as asphalt. It is the SWIR formula that allows the inclusion of wet sand as water to justify the MHWL delineation. Unfortunately, this SWIR band ratio still confused vegetated wetlands because of the feature's combination of high moisture content and green vegetation.

Since the SWIR ratioing was not effective in vegetated wetlands, an NDVI was also employed. First developed by Rouse et al. (1973) and later refined by many including Larsson (1993), NDVI is well known in the literature to be an efficient method to emphasize vegetation while understating non-vegetated surfaces. The NDVI formula was applied to Landsat imagery in the following equation:

$$\frac{(Band4 - Band3)}{(Band4 + Band3)} \qquad \textit{Eq. 5}$$

This ratio of near infrared (Band 4) to red light (Band 3) takes advantage of the fundamental differences between the behavior of each band's spectral range. Near infrared reflects almost entirely off of vegetated surfaces, while red light is absorbed by chlorophyll in vegetation.

After both formulas were applied to the Landsat imagery, a threshold was enforced on each output data layer. This thresholding procedure was invoked to stratify the output layers into categories of either water or land. Thresholds were selected that masked out the greatest area of

NDVI \ SWIR	1	0
1	Land	Land
0	Water	Water

Table 1. Aquatic surface conditional matrix

land while retaining the maximum amount of aquatic surface. The output layers were then reclassified into binary files with aquatic surfaces representing a value of 0 and land representing a value of 1. Finally, a conditional model was created to combine the results of the stratified binary output files for both the SWIR and NDVI processes. In most cases both datasets were in agreement and a clear classification of water or land was made. However, some features were classified as land in one layer and water in the other. In this case, the NDVI surface was used as the default value because its result has overwhelmingly been supported in the literature. The conditional rules are best understood in matrix format (Table 1). The final model output consisted of a single ESRI raster grid containing aquatic surfaces.

3.4. Land Cover Composite

The preceding processing steps resulted in individual data layers for each land cover category. The next analysis procedure was to create one composite dataset of these individual data layers for each time period. Due to time and budgetary constraints there was an absence of field data to validate the classification accuracy of the individual land cover classes. It was assumed that errors of both omission and commission were present in each classification. A composite method was sought that would minimize the compounded error in the final land cover map. An exhaustive review of remote sensing literature provided little guidance in dealing with this lack of accuracy assessment.

As a result, an overlay procedure was designed to combine land cover types into a single land cover map. Confidence scores were assigned to each of the five land cover classification methods based on visual interpretation and literature review. Each thematic category was reclassified to reflect its confidence value. Figure 6 displays the confidence score and subsequent classification value of each land cover type. Errors of commission were reduced by additively overlaying individual land cover classifications with a nested conditional statement in ArcGIS 9.2. For instance, when two coincident cells were evaluated by the conditional model, the more confident raster cell was used in the output. This process reduced the amount of compounded error because less confident data was regularly overwritten by more confident data. This composite method did not address the presumed presence of omission errors.

Confidence Score	Land Cover Class
1	Shrimp Ponds
2	Aquatic Surface
3	Mangrove
4	Sand Dune
5	Salt Flat
6	Upland

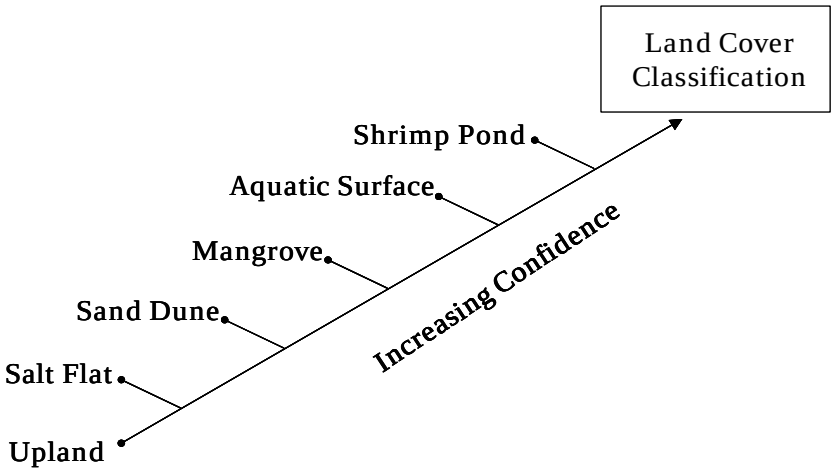

Figure 6. List of confidence scores and a schematic depicting the additive composite procedure

The composite technique was applied to Landsat mosaics for both 1990 and 2000 time periods. Again, a 2006 composite was not generated because complete ASTER imagery coverage was not acquired.

3.5. Change Detection Analysis

Change detection is the process through which changes in the state of a landscape feature are identified by observing it over repeated time intervals (Beland et al. 2006). Lunetta et al. (2002) defined two broad approaches to change detection as pre-classification spectral change detection or post-classification change methods. The latter was employed in this study. According to Jensen (1996), post-classification change detection is the most commonly used quantitative method of change detection. Post-classification change detection consists of overlaying independently produced classifications from different dates to define the state of a pixel through time. Post-classification methods readily lend themselves to a 'from-to' analysis in which information about land cover types are evaluated before and after the change over time.

Post-classification change detection was completed for the northern coast of Northeast Brazil between 1990 and 2000. These separate time period maps were compared on a pixel by pixel basis using a "zip-coding" approach to land cover change detection. Zip-coding allows two different time periods to be represented by a single land cover change code. In this approach, a two-digit land cover change code was assigned to every cell of a raster. The first digit represents a cell's land cover class in 2000 and the second digit represents a cell's class in

1990. For example, if a cell changed from mangrove (class = 3) in 1990 to a shrimp pond (class = 1) in 2000 its land cover change code was '13'. This zip-coding approach resulted in a change image map and a change detection matrix was populated with these values in hectares. Table 2 shows the general logic of a change detection matrix and the individual land cover change codes that will later be replaced by actual values of change (see **4. Results**).

		1990				
		SP	M	SF	SD	AS
2000	SP	**11**	12	13	14	15
	M	21	**22**	23	24	25
	SF	31	32	**33**	34	35
	SD	41	42	43	**44**	45
	AS	51	52	53	54	**55**

Table 2. Change detection matrix with land cover change codes. The boldface diagonal represents areas no change. (SP=shrimp ponds, M=mangrove, SF=salt flat, SD=sand dune, AS=aquatic surface)

Residence stability (RS) is a measure of the rate of change of classes over a given time period of a change detection analysis (Berlanga-Robles & Ruiz-Luna 2006). The conceptually simple residence stability equation was defined in Ramsey et al. (2001) and applied to the change detection matrix for each land cover class in this study:

$$RS = \frac{T_f - T_i}{T_i} * 100$$

where

T_f = land cover class final year area in hectares

T_f = land cover class initial year area in hectares

RS took a negative value when the final year coverage was smaller than the initial year coverage. Positive RS values were present when the land cover class increased relative to the initial year and it was zero when no change was present between 1990 and 2000.

Additional 'from-to' analysis was completed for land cover changes that occurred from 2000 to 2006 as a result of shrimp pond development. Although a complete change detection matrix was not created for this time period, digitized pond boundaries for 2006 were used as a mask to extract the land cover that existed in these locations in 2000.

		1990						
		SP	M	SF	SD	AS	Total (ha)	Total (%)
2000	SP	**31514**	108	894	198	625	33339	11.06
	M	2	**47158**	2298	51	440	49948	16.57
	SF	64	2617	**6421**	4438	1483	15022	4.98
	SD	9	552	1583	**109232**	2936	114312	37.93
	AS	4	430	2822	16344	**69156**	88755	29.45
	Total (ha)	31592	50865	14018	130262	74638	301375	
	Total (%)	10.48	16.88	4.65	43.22	24.77		
	RS (%)	6	-2	7	-12	19		

Table 3. Change detection matrix for land cover changes between 1990 and 2000. (SP=shrimp ponds, M=mangrove, SF=salt flat, SD=sand dune, AS=aquatic surface)

4. Results

Land cover maps and zip-coded time period composites were generated to conduct a change detection analysis. There is no accuracy assessment characterization of these maps because no ground-truthing exercise was conducted. The land cover maps were used to populate the change detection matrix in Table 3. By viewing the diagonal of the change detection matrix it is ascertained that 87% of the classified study area remained unchanged in land cover between 1990 and 2000. The diagonal in the matrix represents all unchanged areas because it is the intersection of the same class for both time periods; all values off the diagonal are considered change. The remaining 13% of land cover change reveals several interesting observations about shrimp aquaculture's impact on the Northeast Brazilian coastal landscape.

For both time periods, sand dune cover dominated the classified portion of the landscape, comprising 43% of the total area in 1990 and 37% in 2000. Surprisingly, sand dunes produced a residence stability (RS) of -12%, indicating that a reduction in this habitat occurred during the time period. An equally surprising land cover trend is the gain of 14,117 new ha of aquatic surface in 2000. The change detection matrix shows a strong interaction between sand dunes and aquatic surfaces, with 78% of lost sand dune being converted to aquatic surface. A total area of 16,344 ha of sand dune was changed to aquatic surfaces.

Mangrove forests proved to be the most stable habitat type in the study area between 1990 and 2000, with an insignificant residence stability of -2%. The only notable transition related to mangroves was a loss of 2,298 ha to the salt flat class in 2000. Salt flats presented the greatest variety of conversion types in land cover from 1990 to 2000. The salt flat class received

significant contributions by mangrove, sand dune and aquatic surface classes to its total area in 2000. The sand dune class was responsible for 52% of the total area of conversion to salt flat in 2000. This transition from other habitats resulted in a residence stability of 7% for salt flats implying there was a meaningful growth in slat flat habitat.

	1990-2000		2000-2006	
	Hectares	% of Total	Hectares	% of Total
M	108	6	63	2
SF	894	49	1581	55
SD	198	11	838	29
AS	625	34	406	14
Total	1825	100	2888	100

Table 4. Land cover converted to shrimp ponds for two different time periods.

The study region experienced some growth of shrimp aquaculture between 1990 and 2000, exhibited by a modest residence stability of 6%. However, between 2000 and 2006 Northeast Brazil underwent a staggering increase in the extent of shrimp pond development (residence stability of 51%). The amount of land utilized by shrimp aquaculture facilities in the region nearly doubled from 33,339ha in 2000 to 50,493ha in 2006. Figure 7 illustrates a typical succession of shrimp pond expansion along Rio Jaguaribe in the Brazilian state of Ceara. Table 4 conveys the land cover classes that were converted to shrimp aquaculture facilities for two different time periods, 1990 to 2000 and 2000 to 2006. As seen in Table 4, only a fraction of the nearly 20,000 ha of new shrimp ponds from 1990 to 2006 are considered in the 'from-to' analysis. A large amount of pond development occurred in areas that were classified as unclassified upland in the previous time period and were omitted from analysis due to a lack of confidence in this land cover category. Of the areas considered, the majority of shrimp pond development occurred in salt flats (49% in 2000 and 55% in 2006). Aquatic surfaces were responsible for 34% of initial habitat conversion in the first time period, but were reduced to

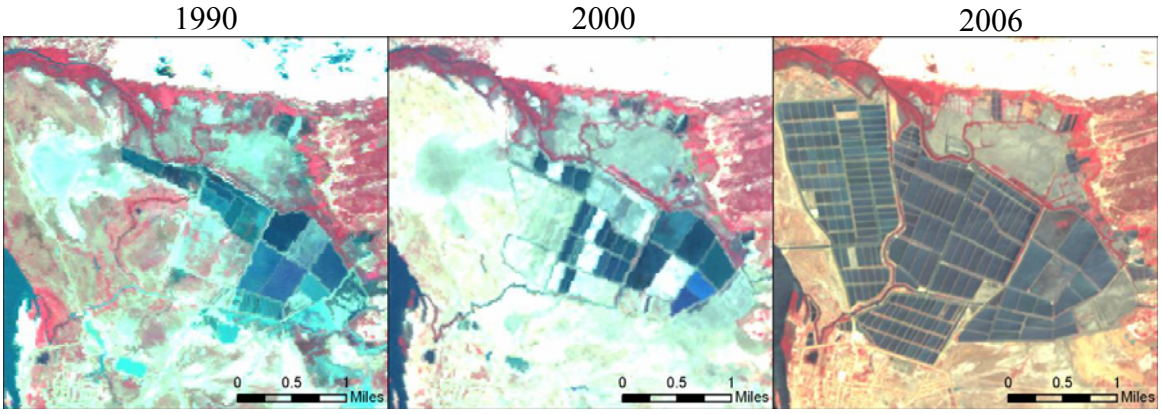

Figure 7. Shrimp pond expansion along Rio Jaguaribe in Ceara state

14% of conversion in the second time period. In keeping with the stability of mangrove forests, only 6% and 2% of total habitat conversion to shrimp ponds occurred in areas that were initially mangrove habitat.

5. Discussion

The results of this study provided leverage to the assertion that shrimp aquaculture development is displacing valuable coastal habitat. However, it is the type of habitat being replaced that has proven most surprising and insightful. The loss of mangrove forests due to shrimp aquaculture expansion has been widely recognized as a major environmental issue throughout the world (Beland et al. 2006, Boyd 2002, Shoobridge 2004, Tong et al. 2004). On the contrary, mangrove forests in Northeast Brazil have exhibited an uncharacteristic stability in a region of heavy shrimp pond development.

Change detection produced a residence stability of -2% for mangrove forests, which was not been determined to be statistically significant. Assuming this slight decrease is significant, two observations can be made about mangroves and pond expansion in the study area. First, direct destruction of mangrove forests is not occurring as this study could only attribute 3% of classified change to the shrimp aquaculture class. Again, this figure is likely well within the margin of error. The second observation implies that if aquaculture is the cause of the 171 ha mangrove loss between 1990 and 2006, it is more probably an indirect effect. Shoobridge (2004) suggested that shrimp aquaculture facilities regularly discharge pond effluents into mangrove forests and will eventually degrade these forests beyond spectral recognition. Another indirect impact may be mangrove degradation due to altered freshwater flow or tidal flooding regime. This speculation about the indirect impacts of shrimp aquaculture on mangroves requires additional investigation beyond remote sensing in order to draw definitive conclusions.

The study also described expansion of salt flat habitat between 1990 and 2000. This finding may be an indication of larger errors in the salt flat classification procedure than in other land cover type classifications undertaken in this study. Expansion of salt flats is counter-intuitive because visual interpretation as well as the statistics presented in Table 4 suggests that salt flats are being targeted for shrimp aquaculture development. Further inspection of the change detection matrix also supports the notion of inadequate salt flat classification. The matrix reports that significant areas of mangrove, aquatic surface and sand dune were converted to salt

flats in 2000. As mentioned earlier, altered tidal flooding regimes and freshwater flows could lead to mangrove degradation or drainage of aquatic surfaces. If shrimp aquaculture induced either of these landscape changes, mangroves or aquatic surfaces could eventually convert to salt flats.

On the other hand, it seems illogical that an area that was once covered by 5-20 m sand dunes will change to salt flat in 10 years. The more likely explanation of this landscape change is a result of classification confusion between salt flats and sand dunes. Recall that salt flats are only inundated by tidal waters 1 to 2 times a month. It is possible that the satellite imagery was acquired during a tidal period when the salt flats were dry and evapotranspiration deposited salt precipitates from the tidal saltwater on the substrate. The precipitate covered salt flat would likely have resembled a sandy surface providing similar spectral signatures for both habitat types. The resulting classification confusion of salt flats in 1990 drastically underestimated salt flat areas and may be the source of a 7% residence stability.

Another illogical land cover change exists for the conversion between sand dune and aquatic surface. The explanation for this conversion is related more to ocean dynamics and not a deficiency in classification methods. The macrotidal regions of Northeast Brazil create expansive river mouths with shifting sand bars. These large sand spits extending from sandy shorelines into river mouths are subject to constant wave action and longshore sediment deposition. Storm events cause sandy areas to give way to surging ocean water. Classified areas exhibiting conversion from sand dune to aquatic surface are simply reflecting this dynamic environment and were not considered alarming landscape conversions.

The margin between classified land cover types and unclassified upland environments proved to be exceedingly problematic in this analysis. Pixels in the study area that were not classified into one of the targeted land cover classes were considered unclassified upland environment. A significant portion of the study area was assigned to the unclassified upland environment in one time period and a classified land cover category in another time period. In interest of providing conservative estimates, these mixed classification pixels were considered to be an error of omission in classification of one time period and were omitted from change detection analysis. This exclusion may have had a large impact on change detection; considering an estimated 253,662 ha were excluded due to mixed classification of this type compared to 301,375 ha of total change detection analysis area. It is likely that some of this excluded area

actually represented meaningful transitions in land cover types. For instance, when all areas of the study area were included, 64% of new shrimp pond development between 1990 and 2000 occurred on unclassified uplands. It is assumed that pond development has occurred in upland areas, but some fraction of the 64% was likely misclassified as upland and is actually one of the targeted land cover types. As a result, it is suggested that total area calculations be evaluated with caution. Instead, percentages of land cover change are safer indicators assuming that the total pixels classified in both time periods are representative of the entire landscape.

6. Conclusion

The goal of this study was to assess the impact of shrimp aquaculture on coastal habitats in Northeast Brazil between 1990 and 2006. Hence a procedure was developed to classify Landsat and ASTER data into land cover maps and conduct post-classification change detection analysis. Without an accuracy assessment incorporating field data for known ground conditions at the time of image acquisition, it is difficult to draw confident conclusions from this study. However in the face of data uncertainty, management decisions regarding Brazil's natural resources must still be made.

The results of this study revealed a substantial growth of shrimp aquaculture facilities on the northern coast of Northeast Brazil between 1990 and 2006. Contrary to literature regarding shrimp aquaculture's impacts in other regions of the world, mangroves are not suffering great losses due to displacement by culture ponds. These low percentages indicated that the least likely location to site new shrimp pond development was in mangrove forests. Surprisingly, it is the expansive tidal salt flats that lie behind mangrove forests that are experiencing the greatest destruction as a result of shrimp aquaculture. Research and management efforts should be directed at determining the extent of utilization of these salt flat areas by migratory shorebirds.

Acknowledgments

The author would like to thank Dr. Patrick Halpin for his facilitation of this Master's Project and exceptionally flexible approach to completion. This research was funded by the United States Fish and Wildlife Service and was supported by Kurt Johnson of FWS. Gary Geller of NASA's Jet Propulsion Lab (JPL) was fundamental in providing satellite imagery and technical understanding of the ASTER sensor. Also, Joe Sexton of Duke University's Nicholas School of the Environment was helpful in his guidance of radiometric correction of the Landsat imagery.

References

Barbosa, L., and Dominguez, J., 2004, Coastal dune fields at the Sao Francisco River strandplain, northeastern Brazil: morphology and environmental controls. *Earth Surface Processes and Landforms*, Vol. 29, No. 4, pp. 443-435.

Beland, M., Goita,K., Bonn, F., and Pham, T.T.H., 2006, Assessment of land-cover changes related to shrimp aquaculture using remote sensing data: a case study in the Giao Thuy District, Vietnam. *International Journal of Remote Sensing*, Vol. 27, No. 8, pp.1491-1510.

Berlanga-Robles, C., and Ruiz-Luna, A., 2006, Assessment of landscape changes and their effects on the San Blas estuarine system, Nayarit (Mexico), through Landsat imagery analysis. *Ciencias Marinas*, Vol. 32, No. 3, pp. 523-538.

Boyd, C., 2002, Mangroves and coastal aquaculture. Responsible Marine Aquaculture, R. Stickney and J. McVey (Eds.)(Wallingford: CABI Publishing), pp. 147-157.

Chander, G. and Markham, B., 2003, Revised Landsat-5 TM Radiometric Calibration Procedures and Postcalibration Dynamic Ranges. *IEEE Transactions on Geoscience and Remote Sensing*, Vol. 41, No. 11, pp. 2674-2677.

Cintron, G., 2006, Biologist U.S. Fish and Wildlife Service, Personal communication.

Cintron, G. and Schaeffer, Y., 2001, An annotated guide to the Ramsar Convention classification system for wetland types: A guide for wetland mangers and planners (Draft), *Proceedings of 9th Meeting of the STRP of Ramsar Convention*.

Daldegan, G.A., Matsumoto, M., and Chatwin, A., 2006, Identificação em nível nacional de tanques de carcinicultura através de imagens obtidas pelo sensor CCD do satélite CBERS-2. (In press).

Earth Satellite Corporation, 2004, Final report: NOAA NOS Special Projects coral reefs, unpublished technical report.

FAO, 2006, State of world aquaculture. FAO Fisheries technical paper, Available online at: ftp://ftp.fao.org/docrep/fao/009/a0874e/a0874e00.pdf.

Green, W., Clark, C., Mumby, P., Edwards, A., and Ellis, A., 1998, Remote sensing techniques for mangrove mapping. *International Journal of Remote Sensing*, Vol. 19, No. 5, pp. 935-956.

Helder, D., Boncyk, W. and Morfitt, R., 1998, Absolute calibration of the Landsat Thematic Mapper using the internal calibrator. *Proceedings of IGARSS, Seattle WA*, pp. 2716-2718.

Jensen, J., 1996, Introductory Digital Image Processing: A Remote Sensing Perspective, 2nd edn. (Upper Saddle River, NJ: Prentice Hill).

Larsson, H., 1993, Regression for canopy cover estimation in Acacia Woodlands using Landsat, TM, MSS, SPOT HRV XS data. *International Journal of Remote Sensing*, Vol. 14, No. 11, pp. 2129-2136.

Lunetta, R., Ediriwickrema, J., Johnson, D., Lyon, J., and McKerrow, A., 2002, Impacts of vegetation dynamics on the identification of land cover change in a biologically complex community in North Carolina, USA. Remote Sensing of Environment, Vol. 82, pp. 258-270.

Markham, B., Seiferth, J., Smid, J., and Barker, J., 1998, Lifetime responsivity behavior of the Landsat-5 Thematic Mapper. *Proceedings of SPIE*, Vol. 3427, pp. 420-431.

Moles, P., and Bunge, J., 2002, Shrimp farming in Brazil: an industry overview. World Bank, NACA, WWF and FAO Consortium on Shrimp Farming and the Environment. Work in Progress for Public Discussion. Published by the Consortium.

NASA, 2007, Landsat 7 science data users' handbook. Available online at: http://landsathandbook.gsfc.nasa.gov/handbook.html

Ramsey III, E., Nelson, G., and Spakota, S., 2001, Coastal change analysis program implemented in Louisiana. *Journal of Coastal Resources*, Vol. 17, pp. 53-71.

Rouse, J., Haas, L., Schell, J., and Deering, D., 1973, Monitoring vegetation systems in the Great Plains with ERTS. *Proceedings of 3rd ERTS Symposium*, Vol. 1, pp.48-62.

Shoobridge, D., 2004, The shrimp farm industry and its impact on the mangrove ecosystem: a case study in Tumbes, Peru. *Proceedings of International Conference of Greening of Industry Network, Hong Kong.*

Song, C., Woodcock, C., Seto, K., Lenney, M., and Macomber, S., 2001, Classification and change detection using Landsat TM data: When and how to correct atmospheric effects?. *Remote Sensing of Environment*, 75, pp. 230-244.

Tong, P., Auda, Y., Populus, J., Aizpuru, M., Habshi, A., and Blasco, F., 2004, Assessment from space of mangroves evolution in the Mekong Delta, in relation to extensive shrimp farming. *International Journal of Remote Sensing*, Vol. 25, No. 21, pp. 4795-4812.

World Bank, NACA, WWF and FAO. 2002. Shrimp Farming and the Environment: To analyze and share experiences on the better management of shrimp aquaculture in coastal areas. Synthesis report. Work in Progress for Public Discussion. Published by the Consortium.

World Wildlife Fund, 2007, Northeastern Brazil restingas (NT0144). Available online at: http://www.nationalgeographic.com/wildworld/profiles/terrestrial/nt/nt0144.html.

Appendices

Appendix 1. Landsat postcalibration dynamic ranges for U.S. processed NLAPS data (Chander & Markham 2003)

Spectral Radiances, $LMIN_\lambda$ and $LMAX_\lambda$ in $W/(m^2.sr.\ \mu m)$								
Processing Date	From March 1, 1984 To May 4, 2003				After May 5, 2003			
Band	$LMIN_\lambda$	$LMAX_\lambda$	$G_{rescale}$	$B_{rescale}$	$LMIN_\lambda$	$LMAX_\lambda$	$G_{rescale}$	$B_{rescale}$
1	-1.52	152.10	0.602431	-1.52	-1.52	193.0	0.762824	-1.52
2	-2.84	296.81	1.175100	-2.84	-2.84	365.0	1.442510	-2.84
3	-1.17	204.30	0.805765	-1.17	-1.17	264.0	1.039880	-1.17
4	-1.51	206.20	0.814549	-1.51	-1.51	221.0	0.872588	-1.51
5	-0.37	27.19	0.108078	-0.37	-0.37	30.2	0.119882	-0.37
6	1.2378	15.303	0.055158	1.2378	1.2378	15.303	0.055158	1.2378
7	-0.15	14.38	0.056980	-0.15	-0.15	16.5	0.065294	-0.15

Appendix 2. Parameter settings for four DOS approaches, DOS1 was utilized in this study (Song et al. 2001)

Methods	T_v	T_z	E_{down}
DOS1	1.0	1.0	0.0
DOS2	1.0	$cos(\theta_z)$	0.0
DOS3	$e^{-\tau v/cos(\theta_v)}$	$e^{-\tau z/cos(\theta_z)}$	Rayleigh(6S)
DOS4	$e^{-\tau v/cos(\theta_v)}$	$e^{-\tau z/cos(\theta_z)}$	πL_p

Appendix 3a. Landsat TM solar exoatmospheric spectral irradiances (Chander & Markham 2003)

Units: ESUN = W/(m^2. μm)		
Model:	**Chance Spectrum CHKUR**	
Band	**Landsat 4**	**Landsat 5**
1	1957	1957
2	1825	1826
3	1557	1554
4	1033	1036
5	214.9	215.0
7	80.72	80.67

Appendix 3b. Landsat ETM+ solar exoatmospheric spectral irradiances (NASA 2007)

Band	watts/(meter squared * μm)
1	1969.000
2	1840.000
3	1551.000
4	1044.000
5	225.700
7	82.07
8	1368.000